Role of event multiplicity on hadronic phase lifetime and QCD phase boundary in ultrarelativistic collisions at energies available at the BNL Relativistic Heavy Ion Collider and CERN Large Hadron Collider

Dushmanta Sahu, Sushanta Tripathy, Girija Sankar Pradhan, and Raghunath Sahoo*
Discipline of Physics, School of Basic Sciences, Indian Institute of Technology Indore, Simrol, Indore 453552, India

(Received 14 September 2019; published 6 January 2020)

Hadronic resonances, having very short lifetimes, like K^{*0}, can act as useful probes to understand and estimate the lifetimes of hadronic phases in ultrarelativistic proton-proton, *p*-Pb, and heavy-ion collisions. Resonances with relatively longer lifetime, like ϕ mesons, can serve as tools to locate the quark-gluon plasma (QGP) phase boundary. We estimate a lower limit of hadronic phase lifetime in Cu-Cu and Au-Au collisions at the Relativistic Heavy Ion Collider (RHIC) and in *pp*, *p*-Pb, and Pb-Pb collisions at different Large Hadron Collider (LHC) collision energies. Also, we obtain the effective temperature of ϕ mesons using the Boltzmann-Gibbs blast-wave function, which gives insight into locating the QGP phase boundary. We observe that the hadronic phase lifetime strongly depends on final-state charged-particle multiplicity, whereas the QGP phase and hence the QCD phase boundary shows very weak multiplicity dependence. This suggests that the hadronization from a QGP state starts at a similar temperature irrespective of charged-particle multiplicity, collision system, and collision energy, while the endurance of hadronic phase is strongly dependent on final-state charged-particle multiplicity, system size, and collision energy.

DOI: 10.1103/PhysRevC.101.014902

I. INTRODUCTION

To reveal the nature of the QCD phase transition and to get a glimpse of how matter behaves at such extreme conditions of temperature and energy density, experiments like the Relativisitic Heavy Ion Collider (RHIC) at BNL, USA, and the Large Hadron Collider (LHC) at CERN, Geneva, Switzerland, have performed hadronic and heavy-ion collisions at ultrarelativistic energies. A deconfined state of quarks and gluons, also known as quark-gluon plasma (QGP), is believed to be produced for a very short time in heavy-ion collisions in these experiments. In the QGP phase, the relevant degrees of freedom are partons: quarks and gluons. In the hadronic phase, composite objects like mesons and baryons are the degrees of freedom [1]. QGP is governed by quantum chromodynamics (QCD) and it is the result of a first-order/cross-over phase transition from normal nuclear matter consisting of mesons and baryons [2,3]. Traditionally, it was believed that for small collision systems, the spacetime evolution could be different than that for heavy-ion collisions. This means that heavy-ion collisions, where the formation of a QGP phase is expected, may undergo various processes like pre-equilibrium of partons, QGP phase, possible mixed phase of partons and hadrons during hadronization, hadronic phase, and finally freeze-out. In contrast, in hadronic collisions, where usually one does not expect the formation of a partonic medium, the system may undergo multiparticle production in the final state, without having a QCD phase transition. The LHC with its unprecedented collision energies has opened up new directions in understanding the possible formation of a QGP medium even in *pp* collisions. Along this direction, the observations of QGP-like properties such as strangeness enhancement [4], double-ridge structure [5], etc., in smaller collision systems like *pp* and *p*-Pb collisions are noteworthy. These developments have important consequences for the results obtained from heavy-ion collisions, as *pp* collisions are used as baseline measurements while characterizing the medium properties in heavy-ion collisions. A closer look at the LHC *pp* collisions, especially the high-multiplicity events, is needed.

There are very few reports on the estimation of hadronic lifetime in *pp* and heavy-ion collisions from either theoretical or experimental prospectives [6]. In this work, we have made an attempt to use short-lived hadronic resonances (like K^{*0}) produced in these collisions to estimate hadronic phase lifetime. In addition, in view of the observed multiplicity scaling at the LHC, we have studied the hadronic phase lifetime as a function of event multiplicity across various collision species like *pp*, *p*-Pb, Cu-Cu, Au-Au, and Pb-Pb collisions for collision energies spanning from GeV to TeV. In contrast, we use long-lived hadronic resonances like ϕ mesons, which have lower hadronic interaction cross sections, to locate the QGP phase boundary in terms of the effective temperature

*Corresponding author: Raghunath.Sahoo@cern.ch

obtained from the Boltzmann-Gibbs blast-wave distribution function. This work would shed light on the role of charged-particle multiplicity, collision system, and collision energy dependence of the partonic and hadronic phases produced at the RHIC and LHC energies.

The paper is organized as follows. The detailed methodology of estimating lifetimes of hadronic phase and location of QGP phase boundary is discussed in the next section. Section III reports the results along with their discussions. Finally, we summarize in Sec. IV with important findings.

II. METHODOLOGY

Before going through the entire procedure to estimate lifetime, let us begin with a brief introduction on evolution of the ultrarelativistic heavy-ion collisions. When two Lorentz contracted nuclei collide at very high energies, the region where they overlap is very thin in the longitudinal direction, much like an almond shape. This energetic interaction results in the formation of a possible state of QGP. QGP exists at very high temperature and/or energy density and consists of asymptotically free quarks and gluons, otherwise known as partons. The created fireball then expands because of very high energy deposition in a small volume with ultrahigh temperature ($\approx 10^5$ times the core of the Sun) and then it cools down until the particles reach a kinetic freeze-out. One can approximately estimate the formation time of the hadrons by the use of the uncertainty principle. The formation time in the rest frame can be related to the hadron size, R_h. In the laboratory frame, the hadron formation time is then given by $t_{\rm form} \simeq R_h \frac{E_h}{m_h}$, where E_h and m_h are the energy and mass of the hadron, respectively [7]. Then, the hadrons start forming inside this QGP medium. After a certain temperature known as the chemical freeze-out temperature ($T_{\rm ch}$), the hadron formation ceases and the stable particle numbers are fixed. At this point, the hadronic phase begins where the produced short-lived resonances decay and the daughter particles undergo multiple rescatterings. After some time, the momentum transfer between the particles also ceases at a temperature called as the kinetic freeze-out temperature ($T_{\rm th}$). Finally all the particles move with relativistic velocities toward the detectors. However, the calculation of QGP and hadronic phase lifetime is not trivial as we can only have the information about the final-state particles in experiments. On the other hand, resonance particles can be used as a probe to calculate the hadronic phase lifetime and locate the QGP phase boundary.

Resonances are usually referred as the particles, which have higher masses than that of the corresponding ground-state particle(s) with similar quark content. As hadronic resonances decay strongly, they have very short lifetime, $\tau \sim$ few fm/c. Before decaying, these particles can only travel up to a few femtometers. The width (Γ) and lifetime (τ) of the resonances are related by the Heisenberg's uncertainty relation, i.e., $\Gamma\tau = \hbar$. As the broad resonance states decay very shortly after their production, it can only be measured by reconstruction of their decay daughters in a detector. The typical lifetimes of experimentally measured hadronic resonances range from 1.1 to 46.2 fm/c. Hadronic resonances

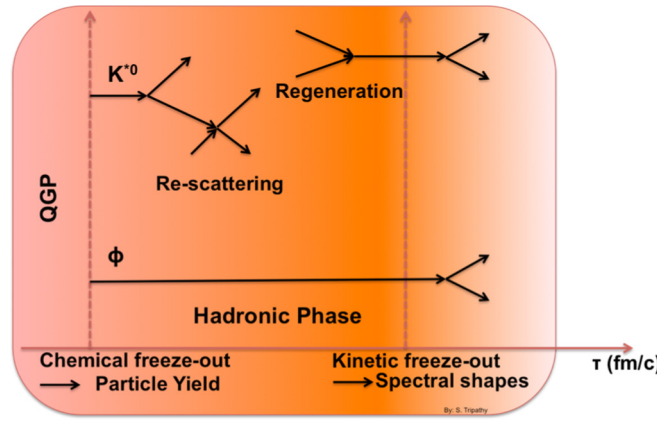

FIG. 1. Depiction of rescattering and regeneration processes of the resonances in the hadronic phase in heavy-ion collisions.

are produced in the bulk of the expanding medium in heavy-ion collisions and they can decay while still traversing in the medium. The decay daughters may interact with other particles in the medium, which would result in suppression of resonances in their reconstruction, as the invariant mass of the daughters may not match with that of the parent particle. This process is known as rescattering. In another way, resonances can be regenerated as a consequence of pseudoelastic collisions in the hadronic phase of the medium, which would result in enhancement of the resonance yields. Resonances, with relatively higher lifetime, might not go through any of the abovementioned processes. It may also happen that the rescattering and regeneration processes compensate for each other. Thus, the interplay of these processes makes the study of resonances in heavy-ion collisions (Fig. 1) more fascinating. As discussed in Ref. [8], the suppression in the ratio of resonances like $\rm K^{*0}/K$ and ρ/π could be due to their late production closer to the kinetic freeze-out.

In Fig. 1, we show the hadronic phase, which starts from chemical freeze-out, where the long-lived particle yields are fixed, to the kinetic freeze-out, where the final-state particle spectra get fixed. We schematically show the rescattering and regeneration processes which might be possible for short-lived resonances like $\rm K^{*0}$, while it is expected that the long-lived resonances like ϕ meson would not go through any of such processes. It is established that the ratio of $\rm K^{*0}$ to K shows significant suppression for central heavy-ion collisions with respect to pp collisions, while ϕ does not go through any such enhancement and/or suppression [9]. This indicates the dominance of rescattering processes over regeneration process in hadronic phase. Depending on the suppression of $\rm K^{*0}$, one can calculate hadronic phase lifetime. For pp low-multiplicity collisions, the $\rm K^{*0}/K$ ratio is taken as the ratio at the chemical freeze-out temperature. The $\rm K^{*0}/K$ ratio at different centralities for different collision systems can be taken as the ratio at the kinetic freeze-out temperature. The lifetime can be calculated using the following relation [10–12],

$$[\rm K^{*0}/K]_{kinetic} = [\rm K^{*0}/K]_{chemical} \times e^{-\Delta t/\tau}, \qquad (1)$$

where τ is the lifetime of K^{*0} and Δt is the hadronic phase lifetime multiplied by the Lorentz factor. The Lorentz factor is calculated using the mean transverse momentum ($\langle p_T \rangle$) of K^{*0}. One could naively expect that the interaction cross section of the decay daughters of K^{*0} (π and K) with other pions in the hadronic phase would be much higher than that of with kaons due to the large relative abundance of pions than kaons. For regeneration, the interaction of πK is essential. So, one would expect that the regeneration effects would be very small compared to rescattering effects. Hence, in our calculation we have neglected the effect of regeneration. Our assumption is supported by the calculations of pion-pion and pion-kaon interactions, where the former interaction cross section is nearly five times larger than that of the latter [13,14]. If there is considerable amount of regeneration of K^{*0}, then the lifetime of hadronic phase would be higher than the calculated lifetime using Eq. (1). Hence, we call the calculated lifetime as the *lower limit* on the hadronic phase lifetime. As the kinetic freeze-out is the time, when all the elastic collisions happen to cease (the mean free path of the system becomes higher than the system size), in a high-multiplicity scenario, because of higher interaction rates due to lower mean free path (particle density being higher), the lifetime of the hadronic phase is expected to be higher as compared to low-multiplicity events. This also justifies the hadronic phase lifetime of heavy-ion collisions being higher than high-multiplicity pp collisions and the latter being again higher than the low-multiplicity events.

Contrary to K^{*0}, ϕ can act as a perfect tool to probe the location of QGP phase boundary. As finding the QGP lifetime is not trivial, we have obtained the temperature ($T_{\rm eff}$) of the system in the QGP phase boundary using the ϕ meson. The ϕ meson is the lightest bound state of a strange and antistrange quark ($s\bar{s}$) and is produced early in the reaction relative to stable particles such as pions, kaons, and protons. It is least affected by hadronic rescattering or regeneration because of its relatively longer lifetime and the decay daughters are expected to decay outside the fireball [15–17]. The results extracted from the analysis of the experimental data on the ratio of various hadronic species [18] indicate that the inelastic interactions of ϕ meson with other hadrons is not significant below the $T_{\rm ch}$. In Refs. [19,20], it has been shown that the ϕN cross section is only around 8–12 mb for photoproduction on proton and nuclear targets below 10 GeV. It has also been shown that out of all ϕ mesons produced, only 5% would rescatter in the hadronic phase of the medium. This in principle should go down as one moves to TeV energies, where the matter is almost baryon free ($\bar{p}/p \sim 0.9$) [21,22]. As the interactions of ϕ meson with other hadrons are very less in the mixed and hadron gas phase, the information of the QGP phase boundary remains intact when ϕ meson is used as a probe. Hence, the transverse momentum spectra of ϕ meson after its hadronization will not be altered or distorted during the expanding hadronic phase. Using the transverse momentum spectra of ϕ, one can obtain reliable information on intensive variables, such as the critical temperature and the location of QGP phase boundary [19,23]. We fit the Boltzmann-Gibbs blast-wave (BGBW) function to the p_T spectra of ϕ meson up to $p_T \sim 3$ GeV/c to get the $T_{\rm th}$, the true freeze-out temperature, and $\langle \beta \rangle$, the average velocity of medium, which can then be used to find out the effective temperature, $T_{\rm eff}$, using the following relation:

$$T_{\rm eff} = T_{\rm th} + \tfrac{1}{2} m \langle \beta \rangle^2. \tag{2}$$

The expression for invariant yield in the BGBW framework is given as follows [24]:

$$E\frac{d^3N}{dp^3} = D\int d^3\sigma_\mu p^\mu \exp\left(-\frac{p^\mu u_\mu}{T}\right). \tag{3}$$

Here, the particle four-momentum is

$$p^\mu = (m_T \cosh y,\, p_T \cos\phi,\, p_T \sin\phi,\, m_T \sinh y). \tag{4}$$

The four-velocity is given as

$$u^\mu = \cosh\rho(\cosh\eta,\, \tanh\rho\cos\phi_r,\, \tanh\rho\sin\phi_r,\, \sinh\eta). \tag{5}$$

The kinetic freeze-out surface is parametrized as

$$d^3\sigma_\mu = (\cosh\eta, 0, 0, -\sinh\eta)\tau r dr d\eta d\phi_r, \tag{6}$$

where η is the space-time rapidity. If we assume Bjorken correlation in rapidity for simplification, i.e., $y = \eta$ [25], Eq. (3) is expressed as

$$\left.\frac{d^2N}{dp_T dy}\right|_{y=0} = D\int_0^{R_0} r\, dr\, K_1\left(\frac{m_T\ \cosh\rho}{T_{\rm th}}\right) I_0\left(\frac{p_T\ \sinh\rho}{T_{\rm th}}\right). \tag{7}$$

Here, D is the normalisation constant, g is the degeneracy factor, and $m_{\rm T} = \sqrt{p_T^2 + m^2}$ is the transverse mass. $K_1(\frac{m_T\ \cosh\rho}{T_{\rm th}})$ and $I_0(\frac{p_T\ \sinh\rho}{T_{\rm th}})$ are the modified Bessel's functions. They are given by

$$K_1\left(\frac{m_T\ \cosh\rho}{T}\right) = \int_0^\infty \cosh y \exp\left(-\frac{m_T\ \cosh y\ \cosh\rho}{T_{\rm th}}\right) dy,$$

$$I_0\left(\frac{p_T\ \sinh\rho}{T}\right) = \frac{1}{2\pi}\int_0^{2\pi} \exp\left(\frac{p_T\ \sinh\rho\ \cos\phi}{T_{\rm th}}\right) d\phi.$$

Here, ρ in the integrand is a parameter given by $\rho = \tanh^{-1}\beta$ and $\beta = \beta_s\,(\xi)^n$ [24,26–28] is the radial flow. Here, β_s is the maximum surface velocity and $\xi = (r/R_0)$, where r is the radial distance. In the BGBW model, the particles closer to the center of the fireball move more slowly than the ones at the edges and the average of the transverse velocity is evaluated as [29]

$$\langle \beta \rangle = \frac{\int \beta_s \xi^n \xi\ d\xi}{\int \xi\ d\xi} = \left(\frac{2}{2+n}\right)\beta_s. \tag{8}$$

For our calculation, we use a linear velocity profile ($n = 1$), and R_0 is the maximum radius of the expanding source at freeze-out ($0 < \xi < 1$).

Keeping the above procedure in mind, let us discuss the results on how final-state multiplicity plays a role in the QGP and hadronic phase lifetime.

III. RESULTS AND DISCUSSION

Figure 2 shows the K^{*0} to K ratio for pp collisions as a function of collision energy for RHIC and LHC. Here we

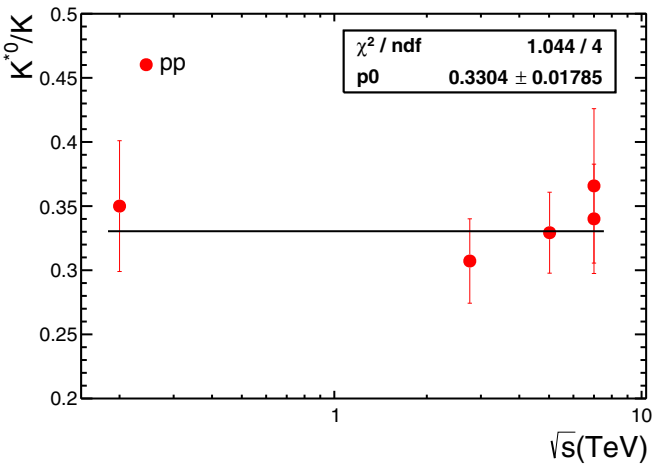

FIG. 2. K^{*0} to K ratio for pp collisions as a function of collision energy. The solid black line shows the fitting of the points with polynomial of order 0.

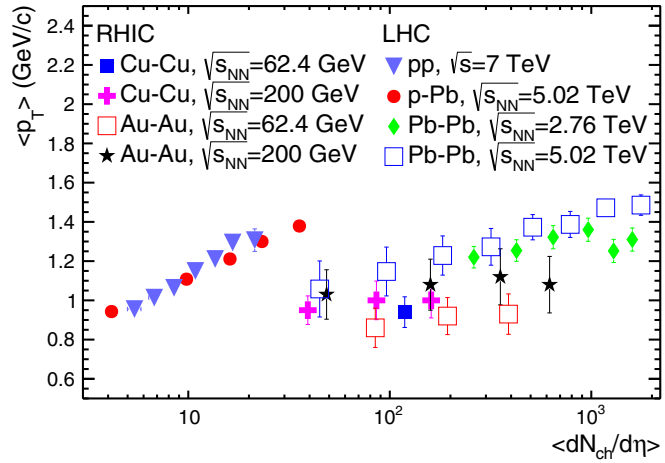

FIG. 4. Mean transverse momentum of K^{*0} for different collision systems as a function of charged-particle multiplicity at different collision energies.

have taken the K^{*0}/K ratios for all the minimum bias pp collisions for different collision energies. In addition, we have also included $\sqrt{s} = 7$ TeV ratio for the low-multiplicity pp collisions. The solid black line shows the fitting of the data points with a zeroth-order polynomial. Assuming this ratio to be the same across all the collision energies, we use $K^{*0}/K = 0.33 \pm 0.02$ as the ratio at the chemical freeze-out in Eq. (1), which is obtained from the above fitting. Figure 3 shows the K^{*0}/K ratio as a function of charged-particle multiplicity for different collision systems at RHIC and LHC [10,12,30–35]. As the data of charged-particle multiplicity, $dN_{ch}/d\eta$ for each centrality class are not available for RHIC energies, we have used Eq. (7) of Ref. [34] (obtained from simultaneous fits) for the conversion from the average number of participants. One should note here that the rapidity range of $dN_{ch}/d\eta$ is $|\eta| < 0.5$ for LHC energies and $|\eta| < 1.0$ for RHIC energies. Clearly, the ratio decreases as a function of charged-particle multiplicity, which suggests significant dominance of

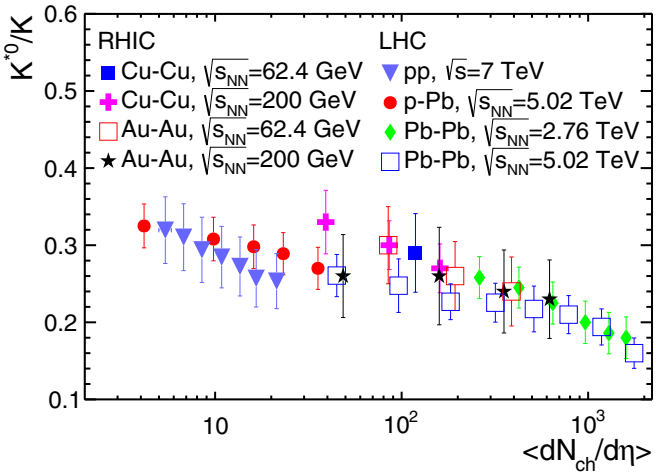

FIG. 3. K^{*0} to K ratio for different collision systems as a function of charged-particle multiplicity.

rescattering effects of the decay daughters over regeneration effects in the hadronic phase. This behavior enables us to use Eq. (1) to obtain the lower limit of the hadronic phase lifetime. For the calculation of the Lorentz factor for hadronic phase lifetime, one needs the mean-transverse momentum ($\langle p_T \rangle$). Figure 4 shows $\langle p_T \rangle$ as a function of charged-particle multiplicity for different collision systems at RHIC and LHC [10,12,30–34]. Clearly, the evolution of $\langle p_T \rangle$ as a function of charged-particle multiplicity does not show smooth evolution across collision systems. The $\langle p_T \rangle$ for small systems like pp and p-Pb collisions have completely different trends than those of heavy-ion collisions. When one moves to higher domain of collision energies, one produces more particles and also the $\langle p_T \rangle$ of the system increases. There seems to be a correlated increase of particle density in phase space and $\langle p_T \rangle$. With same particle density, a higher $\langle p_T \rangle$ would indicate higher collision rate (rescattering) and hence higher hadronic phase lifetime. The calculated hadronic phase lifetime using Eq. (1) shows a linear increase as a function of charged particle multiplicity, as depicted in Fig. 5. This suggests that for a given charged-particle multiplicity, the hadronic phase lifetime is similar irrespective of the collision energy and collision systems for central heavy-ion collisions like Cu-Cu and Au-Au collisions at RHIC and Pb-Pb collisions at the LHC. Peripheral heavy-ion collisions seem to show a different trend, which might be due to the effect of system size and collision energy or, in other words, the effective energy deposited in the Lorentz contracted region [36–39]. However, the small collision systems like pp and p-Pb collisions at the LHC show different evolution compared to heavy-ion collisions. This behavior seems to be propagated from the dependence of $\langle p_T \rangle$ as a function of charged-particle multiplicity although the K^{*0}/K ratio shows a smooth decrease as a function of charged-particle multiplicity. The strong evolution of the lifetime across collision systems and collision energies is clearly visible in the figure. It is observed that the hadronic phase lifetime in high-multiplicity pp collisions is of the order of 2 fm/c, whereas for central Pb-Pb collisions it is around 6 fm/c.

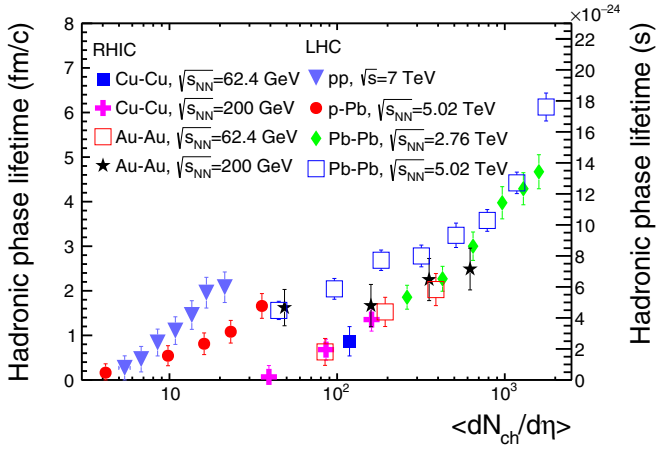

FIG. 5. Hadronic phase lifetime as a function of charged-particle multiplicity for different collision systems at RHIC and LHC energies.

We fit the BGBW as given in Eq. (7) to the p_{T} spectra of ϕ meson in different multiplicity classes to get the T_{th}, the true freeze-out temperature and $\langle\beta\rangle$, the average radial flow velocity of medium. Figure 6 shows the blast-wave fit for p_{T} spectra in Pb-Pb collisions at $\sqrt{s_{NN}} = 2.76$ TeV for different centrality classes. Similarly, Figs. 7 and 8 show the blast-wave fit for p_{T} spectra in p-Pb collisions at $\sqrt{s_{NN}} = 5.02$ TeV and in pp collisions at $\sqrt{s} = 7$ TeV for different multiplicity classes, respectively. The fitting is performed upto $p_{\mathrm{T}} = 3$ GeV/c. The lower panels show the fit to data ratio for different collision systems. The fit quality seems reasonable as the maximum deviation of fit does not exceed beyond 10% for Pb-Pb, p-Pb, and high-multiplicity pp collisions. As expected, the fit quality is worse for the low-multiplicity pp collisions

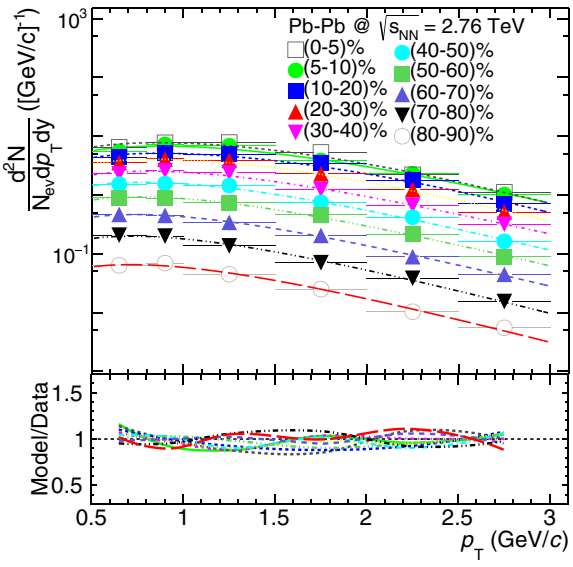

FIG. 6. Fitting of Boltzmann-Gibbs Blast-Wave distribution to p_{T} spectra of ϕ meson production in Pb-Pb collisions at $\sqrt{s_{NN}} = 2.76$ TeV.

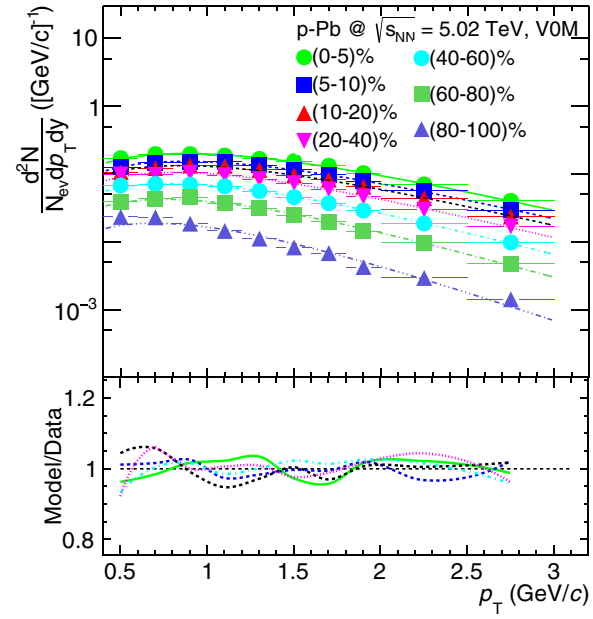

FIG. 7. Fitting of Boltzmann-Gibbs blast-wave distribution to p_{T} spectra of ϕ meson production in p-Pb collisions at $\sqrt{s_{NN}} = 5.02$ TeV.

due to less probable blast-wave scenario in low-multiplicity pp collisions.

From these fits, we find the values of $\langle\beta\rangle$ and T_{th} for all collision systems in different centralities. By using these values in Eq. (2), we can find the effective temperature (T_{eff}) of ϕ mesons. Figure 9 shows the kinetic freeze-out temperature for ϕ meson, denoted by T_{th}, as a function of charged-particle multiplicity. One can observe that the temperature shows almost a flat trend up to a certain $dN_{\mathrm{ch}}/d\eta$ and then drops immediately afterward. This can be explained by considering

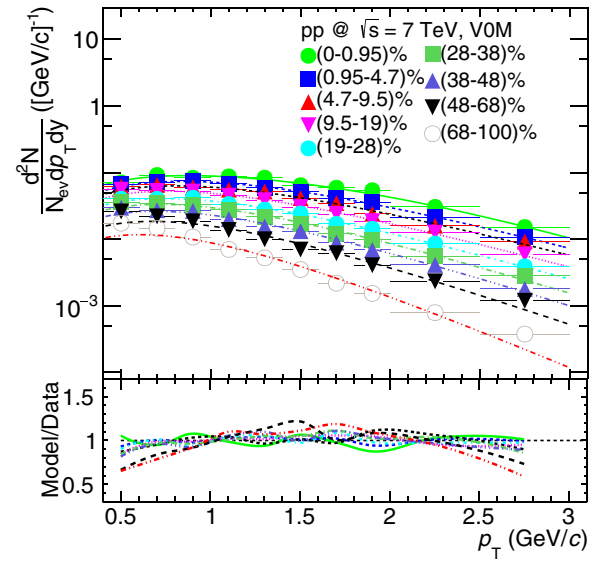

FIG. 8. Fitting of Boltzmann-Gibbs blast-wave distribution to p_{T} spectra of ϕ meson production in pp collisions at $\sqrt{s} = 7$ TeV.

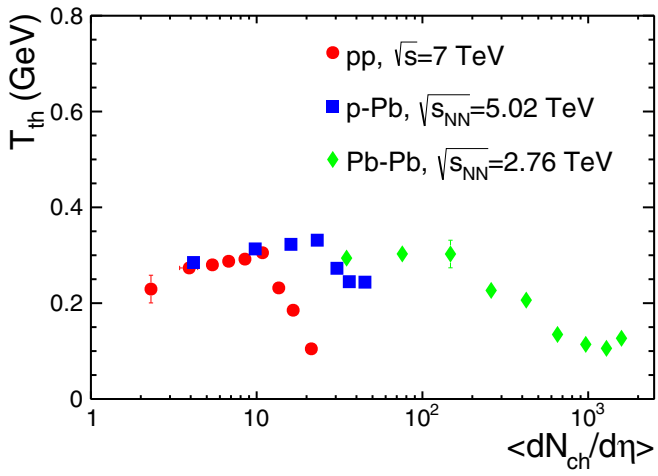

FIG. 9. Kinetic freeze-out temperature for ϕ meson as a function charged-particle multiplicity for different collision systems.

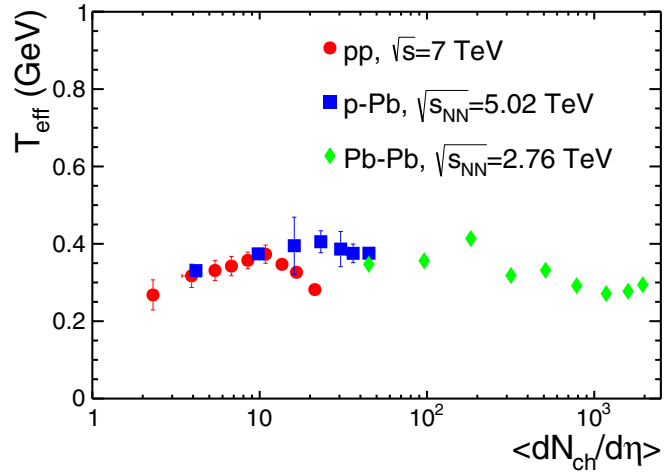

FIG. 11. Effective temperature for ϕ meson as a function charged-particle multiplicity for different collision systems.

the fact that for low charged-particle multiplicity, the system freezes out early, means it freezes out at high $T_{\rm th}$. As the charged-particle multiplicity becomes more, the system is thought to have gone through a QGP phase, which results in the system taking a longer time to attain the kinetic freeze-out. This is also evident from our findings of higher hadronic phase lifetime for high-multiplicity collisions. As a result, the kinetic freeze-out temperature drops abruptly in all the collision systems. We observe that the drop of $T_{\rm th}$ happens at different charged-particle multiplicities in different collision systems. Figure 10 shows the average radial flow as a function of charged-particle multiplicity for different collision systems at the LHC. It can be seen that $\langle\beta\rangle$ increases smoothly in all the collision systems up to a certain extent. However, for pp collisions at a certain charged-particle multiplicity ($\simeq$10–20), $\langle\beta\rangle$ shows a sudden increase. Observation of this threshold in the final-state charged particle multiplicity is supported by the following additional observations for a change in dynamics of the system. $N_{\rm ch} \simeq$ 10–20 has been found to be

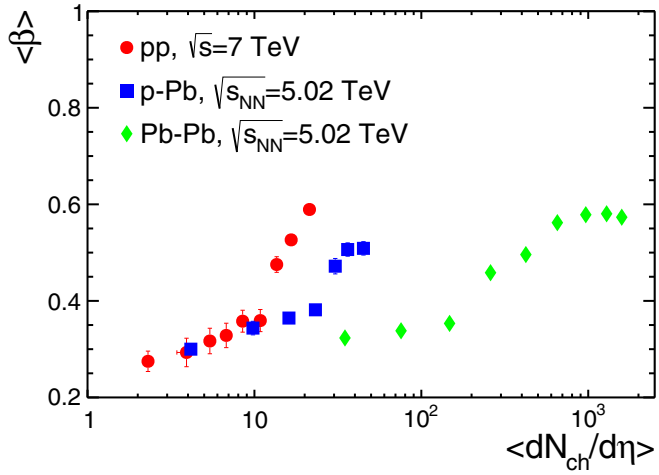

FIG. 10. Average radial flow for ϕ meson as a function charged-particle multiplicity for different collision systems.

a limit after which the multipartonic interactions (MPI) in pp collisions is found to show an important role in particle production (quarkonia) at the LHC energies [40]. In addition, this threshold is also supported as a thermodynamic limit after which all the statistical ensembles give similar results while describing the freeze-out properties of the system [41]. After this threshold, we have also observed $T_{\rm ch}$ to be higher than the kinetic freeze-out temperature [42]. We know that the average radial flow is larger for a system that goes through QGP phase. Again, this suggests a higher probability of QGP formation after this particular charged-particle multiplicity which may have been the reason for the sudden increase in $\langle\beta\rangle$. The behavior of $\langle\beta\rangle$ complements the results observed in Fig. 9. This again is supported by earlier predictions for a cross-over transition from hadronic to QGP phase to happen between charged particle multiplicity density of 6 to 24 [43].

Figure 11 shows the effective temperature of ϕ meson as a function of charged-particle multiplicity, which encodes the temperature due to thermal motion ($T_{\rm th}$) and due to the collective motion (calculated from $\langle\beta\rangle$). It is clearly seen that regardless of the collision systems, $T_{\rm eff}$ does not show any major dependence on $dN_{\rm ch}/d\eta$. This behavior is unlike the behaviors observed for $T_{\rm th}$ and $\langle\beta\rangle$ as a function of charged-particle multiplicity. As ϕ meson keeps the information of QGP phase boundary intact, the trend of $T_{\rm eff}$ suggests that the location of QGP phase boundary is independent or weakly dependent on charged particle multiplicity. Interestingly, this observation is also supported by earlier reports of $T_{\rm ch}$ being independent of final-state charged particle multiplicity [42].

Figures 5 and 11 suggest that the hadronic phase lifetime strongly depends on charged-particle multiplicity while the QGP phase shows very weak dependence on charged-particle multiplicity. This indicates that the hadronization from a QGP state starts at a similar temperature irrespective of charged-particle multiplicity, collision system, and collision energy while the duration of the hadronic phase strongly depends on final-state charge-particle multiplicity.

IV. SUMMARY

In this work, we have made an attempt to use hadronic resonances produced in *pp*, *p*-Pb, Cu-Cu, Au-Au, and Pb-Pb collisions to have an estimation of hadronic phase lifetime and to locate the QGP phase boundary. In summary, the following are our main points:

(1) For a given charged-particle multiplicity, the hadronic phase lifetime is similar irrespective of the collision energy and collision systems for central heavy-ion collisions like Cu-Cu and Au-Au collisions at RHIC and Pb-Pb collisions at the LHC. Peripheral heavy-ion collisions seem to show a different behavior, which could be because of the effect of system size and collision energy or, in brief, the effective energy responsible for particle production. However, the small collision systems like *pp* and *p*-Pb collisions at the LHC show different evolution compared to heavy-ion collisions. This behavior seems to be propagated from the dependence of $\langle p_{\mathrm{T}} \rangle$ as a function of charged-particle multiplicity although the $\mathrm{K}^{*0}/\mathrm{K}$ shows a smooth decrease as a function of charged-particle multiplicity.

(2) We observe that the hadronic phase lifetime strongly depends on final-state charged-particle multiplicity, system size, and collision energy, while the QGP phase show very weak dependence on charged-particle multiplicity.

(3) This suggests that the hadronization from a QGP state starts at a similar temperature, which seems to be independent of charged-particle multiplicity, collision system, and collision energy while the lifetime of hadronic phase is strongly dependent of final-state charge-particle multiplicity.

(4) The abrupt change in behavior of kinetic freeze-out temperature and average radial flow for *pp* collisions after certain charged-particle multiplicity ($\simeq$10–20) suggests that the charged-particle multiplicity $\simeq$10–20 could act as minimum requirement of QGP formation.

In view of the discovery of hints of QGP droplets in small collision systems at the LHC [44], this work sheds light onto the role of event multiplicity on the formation of a deconfined phase and the lifetime of hadronic phase produced in various ultrarelativistic collisions. A clearer picture may emerge if the exact lifetime of QGP can be estimated for different charged-particle multiplicities, which is still an open problem. In this direction, the effective energy that is responsible for particle production, which in principle controls the final-state multiplicity, may be the responsible factor, which needs further exploration [36–39].

ACKNOWLEDGMENTS

The authors acknowledge the financial support from ALICE Project No. SR/MF/PS-01/2014-IITI(G) of the Department of Science and Technology, Government of India. S.T. and G.S.P. acknowledge the financial support by the DST-INSPIRE program of the Goverment of India.

[1] Y. Aoki, G. Endrodi, Z. Fodor, S. D. Katz, and K. K. Szabo, Nature (London) **443**, 675 (2006).
[2] J. W. Harris and B. Muller, Ann. Rev. Nucl. Part. Sci. **46**, 71 (1996).
[3] P. Braun-Munzinger and J. Stachel, Nature (London) **448**, 302 (2007).
[4] J. Adam *et al.* (ALICE Collaboration), Nat. Phys. **13**, 535 (2017).
[5] V. Khachatryan *et al.* (ALICE Collaboration), Phys. Lett. B **765**, 193 (2017).
[6] R. Rapp and H. van Hees, Phys. Lett. B **753**, 586 (2016).
[7] K. Adcox *et al.* (PHENIX Collaboration), Nucl. Phys. A **757**, 184 (2005).
[8] R. Rapp, Nucl. Phys. A **725**, 254 (2003).
[9] B. B. Abelev *et al.* (ALICE Collaboration), Phys. Rev. C **91**, 024609 (2015).
[10] J. Adams *et al.* (ALICE Collaboration), Phys. Rev. C **71**, 064902 (2005).
[11] S. Singha, B. Mohanty, and Z. W. Lin, Int. J. Mod. Phys. E **24**, 1550041 (2015).
[12] S. Acharya *et al.* (ALICE Collaboration), arXiv:1910.14419 [nucl-ex].
[13] M. J. Matison, A. Barbaro-Galtieri, M. Alston-Garnjost, S. M. Flatte, J. H. Friedman, G. R. Lynch, M. S. Rabin, and F. T. Solmitz, Phys. Rev. D **9**, 1872 (1974).
[14] S. D. Protopopescu *et al.*, Phys. Rev. D **7**, 1279 (1973).
[15] C. M. Ko and D. Seibert, Phys. Rev. C **49**, 2198 (1994).
[16] K. Haglin, Nucl. Phys. A **584**, 719 (1995).
[17] R. Sahoo, T. K. Nayak, J. E. Alam, B. K. Nandi, and S. Kabana, Int. J. Mod. Phys. A **26**, 4145 (2011).
[18] P. Braun-Munzinger, K. Redlich, and J. Stachel, in *Quark-Gluon Plasma 3*, edited by R. C. Hwa and X.-N. Wang (World Scientific, Singapore, 2004), pp. 491–599.
[19] A. Shor, Phys. Rev. Lett. **54**, 1122 (1985).
[20] A. Sibirtsev, H. W. Hammer, U. G. Meissner, and A. W. Thomas, Eur. Phys. J. A **29**, 209 (2006).
[21] K. Aamodt *et al.* (ALICE Collaboration), Phys. Rev. Lett. **105**, 072002 (2010).
[22] A. Tawfik, Nucl. Phys. A **859**, 63 (2011).
[23] M. Nasim, V. Bairathi, M. K. Sharma, B. Mohanty, and A. Bhasin, Adv. High Energy Phys. **2015**, 197930 (2015).
[24] E. Schnedermann, J. Sollfrank, and U. W. Heinz, Phys. Rev. C **48**, 2462 (1993).
[25] J. D. Bjorken, Phys. Rev. D **27**, 140 (1983).
[26] P. Huovinen, P. F. Kolb, U. W. Heinz, P. V. Ruuskanen, and S. A. Voloshin, Phys. Lett. B **503**, 58 (2001).
[27] P. Braun-Munzinger, J. Stachel, J. P. Wessels, and N. Xu, Phys. Lett. B **344**, 43 (1995).
[28] Z. Tang *et al.*, Chin. Phys. Lett. **30**, 031201 (2013).
[29] K. Adcox *et al.* (PHENIX Collaboration), Phys. Rev. C **69**, 024904 (2004).
[30] M. M. Aggarwal *et al.* (ALICE Collaboration), Phys. Rev. C **84**, 034909 (2011).

[31] S. Acharya *et al.* (ALICE Collaboration), Phys. Rev. C **99**, 024906 (2019).
[32] J. Adam *et al.* (ALICE Collaboration), Phys. Rev. C **95**, 064606 (2017).
[33] J. Adam *et al.* (ALICE Collaboration), Eur. Phys. J. C **76**, 245 (2016).
[34] B. Alver *et al.* (PHOBOS Collaboration), Phys. Rev. C **83**, 024913 (2011).
[35] S. Tripathy (ALICE Collaboration), Nucl. Phys. A **982**, 180 (2019).
[36] A. N. Mishra, R. Sahoo, E. K. G. Sarkisyan, and A. S. Sakharov, Eur. Phys. J. C **74**, 3147 (2014); Erratum: **75**, 70 (2015).
[37] E. K. G. Sarkisyan, A. N. Mishra, R. Sahoo, and A. S. Sakharov, Phys. Rev. D **93**, 054046 (2016); **93**, 079904(E) (2016).
[38] E. K. G. Sarkisyan, A. N. Mishra, R. Sahoo, and A. S. Sakharov, Phys. Rev. D **94**, 011501(R) (2016).
[39] E. K. Sarkisyan-Grinbaum, A. Nath Mishra, R. Sahoo, and A. S. Sakharov, Europhys. Lett. **127**, 62001 (2019).
[40] D. Thakur, S. De, R. Sahoo, and S. Dansana, Phys. Rev. D **97**, 094002 (2018).
[41] N. Sharma, J. Cleymans, B. Hippolyte, and M. Paradza, Phys. Rev. C **99**, 044914 (2019).
[42] R. Rath, A. Khuntia, and R. Sahoo, arXiv:1905.07959 [hep-ph].
[43] R. Campanini and G. Ferri, Phys. Lett. B **703**, 237 (2011).
[44] R. Sahoo, AAPPS Bull. **29**, 16 (2019).